

Photoassociation spectra and the validity of the dipole approximation for weakly bound dimers

Daniel G. Cocks¹ and Ian B. Whittingham¹

¹*School of Engineering and Physical Sciences, James Cook University, Townsville, Australia 4811*
(Dated: June 4, 2018)

Photoassociation (PA) of ultracold metastable helium to the $2s2p$ manifold is theoretically investigated using a non-perturbative close-coupled treatment in which the laser coupling is evaluated without assuming the dipole approximation. The results are compared with our previous study [Cocks and Whittingham, *Phys. Rev. A* **80**, 023417 (2009)] that makes use of the dipole approximation. The approximation is found to strongly affect the PA spectra because the photoassociated levels are weakly bound, and a similar impact is predicted to occur in other systems of a weakly bound nature. The inclusion or not of the approximation does not affect the resonance positions or widths, however significant differences are observed in the background of the spectra and the maximum laser intensity at which resonances are discernable. Couplings not satisfying the dipole selection rule $|J - 1| \leq J' \leq |J + 1|$ do not lead to observable resonances.

PACS numbers: 32.70.Jz, 34.50.Cx, 34.50.Rk, 34.20.Cf

I. INTRODUCTION

Photoassociation (PA) is a powerful technique exploited by researchers to probe the fundamental interactions of ultracold quantum gases [1, 2]. Of particular interest is PA in metastable helium where release of the large internal energy during collisions provides unique experimental investigation strategies. We have recently analysed the PA process [3] and obtained detailed information of the laser intensity dependence of the line shifts and widths of the resonance peaks in the PA spectra of ultracold metastable helium excited to the $J = 1, 0_u^+$ rovibrational states in the $2^3S_1 + 2^3P_0$ asymptote. Two variants of a full nonperturbative multichannel, close-coupled treatment were used to obtain the required scattering matrix \mathcal{S} in the presence of the non-vanishing asymptotic radiative coupling, one based upon dressed states, and the other on a modified radiative coupling that vanishes asymptotically. Although both methods gave nearly identical results for the line shifts and widths, these peaks were superimposed on very significant backgrounds that differed, especially at higher laser intensities. These significant backgrounds are a direct consequence of the weakly bound nature of the excited levels in metastable helium and are not found in PA studies of other systems.

In common with all previous investigations of PA in ultracold gases, we assumed the dipole approximation in evaluating the matrix elements of the laser coupling. However, in light of the sensitivity of the background radiation loss to the form of the radiative coupling at large distances, we revisit the validity of this approximation and its applicability to weakly bound levels in general.

The laser coupling term is given by

$$\hat{H}_{\text{int}} = -\left(\frac{e}{m}\right) \sum_{i=1,2} \hat{\mathbf{p}}_i \cdot \hat{\mathbf{A}}(\mathbf{r}_i) \quad (1)$$

where $\hat{\mathbf{p}}_i = -i\hbar\nabla_{\mathbf{r}_i}$ and the vector potential at the po-

sition \mathbf{r}_i of the i th electron is

$$\hat{\mathbf{A}}(\mathbf{r}_i) = \sum_{\xi} [\mathcal{E}_{\xi}(\mathbf{r}_i) \hat{a}_{\xi} + \mathcal{E}_{\xi}(\mathbf{r}_i)^* \hat{a}_{\xi}^{\dagger}]. \quad (2)$$

Here \hat{a}_{ξ}^{\dagger} (\hat{a}_{ξ}) are the creation (annihilation) operators for a photon of angular frequency ω_{ξ} and polarization $\boldsymbol{\epsilon}_{\xi}$ and

$$\mathcal{E}_{\xi}(\mathbf{r}_i) = \sqrt{\frac{\hbar}{2\omega_{\xi}\epsilon_0\mathcal{V}}} e^{i\mathbf{k}\cdot\mathbf{r}_i} \boldsymbol{\epsilon}_{\xi}, \quad (3)$$

where \mathbf{k} is the wave-vector of the laser field, e and m are the electron charge and mass respectively and \mathcal{V} is the normalization volume. The dipole approximation makes the assumption that $\exp(i\mathbf{k}\cdot\mathbf{r}_i) \approx 1$. If the laser coupling is only significant in the region of the excited rovibrational states this is a reasonable assumption to make, as the outer turning points of the ultra long-range $J = 1, 0_u^+$ vibrational states of this investigation place an upper bound of $r_i < R/2 < 235 a_0$, where R is the interatomic distance. Since $k = 1/3258.17 a_0^{-1}$ for the $2s^3S - 2p^3P$ transition, this gives $0.92 < |\exp(i\mathbf{k}\cdot\mathbf{r}_i)| < 1.08$.

The multichannel calculation of our previous investigation, however, involves open channels of the metastable basis coupled to the excited state, and the S -matrix elements and loss profiles were obtained by matching the asymptotic forms of the open channels at distances $R > 10^5 a_0$, much greater than the interatomic ranges of the vibrational states. The coupling to the excited state, even at very large ranges where the uncoupled bound wavefunction was negligible, still influenced the calculation due to the closeness of the bound levels to the excited state dissociation limit. This influence can be suppressed and the background to the PA spectra removed by artificially deepening the potential well. The presence of this background introduced new features such as the elimination of resonance peaks by saturation of the laser intensity, and it is evident that the laser coupling must be treated more carefully in non-perturbative calculations of PA profiles.

The validity of the dipole approximation at large interatomic separations of $O(10^5) a_0$ is questionable, at least when weakly bound levels are considered. In this paper we study the effects of the non-dipole contributions to the PA spectra in metastable helium by firstly deriving an expression for the matrix elements of the laser coupling which fully includes the $\exp(i\mathbf{k} \cdot \mathbf{r}_i)$ factors and then re-do the multichannel calculations of [3] using these matrix elements.

It is worth noting that the exponential term that is ignored in the dipole approximation has the effect of introducing a momentum transfer from the absorbed photon to the molecule. For ultracold atoms this momentum transfer can be much larger than the initial momentum of the colliding atoms.

II. EXACT LASER COUPLING

A. General form

The close-coupled equations for the two colliding atoms in the applied laser field involve the matrix elements of the laser coupling operator, \hat{H}_{int} between basis states of the general form

$$|\Psi_g\rangle \equiv R^{-1}G_g(R)|g\rangle|n, \omega, \epsilon_\lambda\rangle \quad (4)$$

and

$$|\Psi_e\rangle \equiv R^{-1}G_e(R)|e\rangle|n-1, \omega, \epsilon_\lambda\rangle. \quad (5)$$

Here the molecular basis states $|a\rangle$, where $a = \{g, e\}$, are assumed to have no dependence upon the interatomic distance R but may still depend upon the molecular orientation in the space-fixed frame, specified by the angles (θ, ϕ) , and the electronic coordinates \mathbf{r}_i . The laser field states are denoted by $|n, \omega, \epsilon_\lambda\rangle$, representing n photons of frequency ω and polarization ϵ_λ , where $\lambda = 0, \pm 1$ for π, σ^\pm polarization. We assume the laser is directed along the space-fixed Oz -axis.

We consider the matrix element

$$V_{eg}^{\text{int}} \equiv \langle e|\langle n-1, \omega, \epsilon_\lambda|\hat{H}_{\text{int}}|g\rangle|n, \omega, \epsilon_\lambda\rangle. \quad (6)$$

As only the term involving the annihilation operator \hat{a}_ξ contributes, we have

$$V_{eg}^{\text{int}} = -\frac{e}{m}\sqrt{\frac{n\hbar}{2\omega\epsilon_0\mathcal{V}}}\langle e|\sum_i(\hat{\mathbf{p}}(\mathbf{r}_i) \cdot \epsilon_\lambda)e^{i\mathbf{k} \cdot \mathbf{r}_i}|g\rangle \quad (7)$$

where

$$\langle n-1, \omega, \epsilon_\lambda|\hat{a}_\xi|n, \omega, \epsilon_\lambda\rangle = \delta_{\lambda\xi}\sqrt{n} \quad (8)$$

has been used.

Evaluation of (7) requires the choice of a coordinate system. We specify the origin of the coordinate system to be the center of mass of the dimer (assumed to consist

of identical nuclei), such that the position of nucleus A is given by $-\mathbf{R}/2$ and nucleus B by $\mathbf{R}/2$. The electron coordinates \mathbf{r}_i can then be expressed as $\mathbf{r}_i = \hat{\eta}_i\mathbf{R}/2 + \mathbf{r}'_i$ where the operator $\hat{\eta}_i$ has eigenvalues of ∓ 1 if electron i is centered upon atom A or B respectively, and \mathbf{r}'_i is the position vector of electron i with origin at its respective atom. Similarly, the momentum operators become $\hat{\mathbf{p}}(\mathbf{r}_i) = \hat{\eta}_i\hat{\mathbf{p}}(\mathbf{R})/2 + \hat{\mathbf{p}}(\mathbf{r}'_i)$.

The matrix element (7) then becomes

$$V_{eg}^{\text{int}} = -\frac{e}{m}\sqrt{\frac{n\hbar}{2\omega\epsilon_0\mathcal{V}}}\sum_i\langle e|\left[\hat{\eta}_i\frac{1}{2}\hat{\mathbf{p}}(\mathbf{R}) + \hat{\mathbf{p}}(\mathbf{r}'_i)\right] \cdot \epsilon_\lambda \times e^{\hat{\eta}_i i\mathbf{k} \cdot \mathbf{R}/2} e^{i\mathbf{k} \cdot \mathbf{r}'_i}|g\rangle. \quad (9)$$

This expression can be simplified by separating the basis states into a rotational part which depends only upon (θ, ϕ) and the electronic part that is independent of \mathbf{R} :

$$|a\rangle = |\psi_a^{\text{rot}}\rangle|\psi_a^{\text{el}}\rangle. \quad (10)$$

After action of the momentum operators, the matrix element $\langle e|\dots|g\rangle$ inside the summation becomes

$$\begin{aligned} & \langle \psi_e^{\text{rot}}|\frac{i\hat{\eta}_i^2\mathbf{k} \cdot \epsilon_\lambda}{4}e^{\hat{\eta}_i i\mathbf{k} \cdot \mathbf{R}/2}\langle \psi_e^{\text{el}}|e^{i\mathbf{k} \cdot \mathbf{r}'_i}|\psi_g^{\text{el}}\rangle|\psi_g^{\text{rot}}\rangle \\ & + \langle \psi_e^{\text{rot}}|\frac{\hat{\eta}_i}{2}e^{\hat{\eta}_i i\mathbf{k} \cdot \mathbf{R}/2}\langle \psi_e^{\text{el}}|e^{i\mathbf{k} \cdot \mathbf{r}'_i}|\psi_g^{\text{el}}\rangle\hat{\mathbf{p}}(\mathbf{R}) \cdot \epsilon_\lambda|\psi_g^{\text{rot}}\rangle \\ & + \langle \psi_e^{\text{rot}}|e^{\hat{\eta}_i i\mathbf{k} \cdot \mathbf{R}/2}\langle \psi_e^{\text{el}}|i(\mathbf{k} \cdot \epsilon_\lambda)e^{i\mathbf{k} \cdot \mathbf{r}'_i}|\psi_g^{\text{el}}\rangle|\psi_g^{\text{rot}}\rangle \\ & + \langle \psi_e^{\text{rot}}|e^{\hat{\eta}_i i\mathbf{k} \cdot \mathbf{R}/2}\langle \psi_e^{\text{el}}|e^{i\mathbf{k} \cdot \mathbf{r}'_i}\hat{\mathbf{p}}(\mathbf{r}'_i)|\psi_g^{\text{el}}\rangle \cdot \epsilon_\lambda|\psi_g^{\text{rot}}\rangle. \end{aligned} \quad (11)$$

The first and third terms are zero since $\mathbf{k} \cdot \epsilon_\lambda = 0$. In the second and fourth terms we can assume $\exp(i\mathbf{k} \cdot \mathbf{r}'_i) \approx 1$ as the inner product $\langle \psi_e^{\text{el}}|\dots|\psi_g^{\text{el}}\rangle$ is non-negligible with respect to \mathbf{r}'_i only in the regions of the atomic electrons. As such, the second term is also zero because the ground and excited states are orthogonal.

To proceed, we use the expansion for a plane wave in terms of Legendre polynomials

$$\begin{aligned} e^{\hat{\eta}_i i\mathbf{k} \cdot \mathbf{R}/2} &= \sum_p i^p(2p+1)j_p(kR/2)P_p(\hat{\eta}_i \cos \theta) \\ &= \sum_p i^p(2p+1)j_p(kR/2)(\hat{\eta}_i)^p D_{00}^{p*} \end{aligned} \quad (12)$$

where $D_{m'm}^j \equiv D_{m'm}^j(\phi, \theta, 0)$ is a Wigner rotation matrix [5]. Recalling the equality $e\hat{\mathbf{p}}(\mathbf{r}'_i)/m = i[\hat{H}_{\text{mol}}, \hat{\mathbf{d}}^i]/\hbar$, where $\hat{\mathbf{d}}^i = e\mathbf{r}_i$ is the atomic dipole operator for electron i , the matrix element becomes

$$\begin{aligned} V_{eg}^{\text{int}} &= -\sqrt{\frac{n}{2\hbar\omega\epsilon_0\mathcal{V}}}\sum_{i,p}\langle \psi_e^{\text{rot}}|i^{p+1}(2p+1)j_p(kR/2)D_{00}^{p*} \\ & \quad \times \langle \psi_e^{\text{el}}|(\hat{\eta}_i)^p [\hat{H}_{\text{mol}}, \hat{\mathbf{d}}^i]|\psi_g^{\text{el}}\rangle \cdot \epsilon_\lambda|\psi_g^{\text{rot}}\rangle \\ &= -\sqrt{\frac{n\hbar\omega}{2\epsilon_0\mathcal{V}}}\sum_{i,p}\langle \psi_e^{\text{rot}}|i^{p+1}(2p+1)j_p(kR/2)D_{00}^{p*} \\ & \quad \times \langle \psi_e^{\text{el}}|(\hat{\eta}_i)^p \hat{\mathbf{d}}^i|\psi_g^{\text{el}}\rangle \cdot \epsilon_\lambda|\psi_g^{\text{rot}}\rangle. \end{aligned} \quad (13)$$

In obtaining (13) we have assumed the difference between electronic energies $E_e - E_g$ is approximately $\hbar\omega$.

The matrix element of \hat{d}^i is most easily evaluated in the molecular frame using spherical tensors. The expansion required is

$$\begin{aligned}\hat{d}^i \cdot \epsilon_\lambda &= \sum_\mu (-1)^\mu (\epsilon_\lambda)_{-\mu} \hat{d}_\mu^i \\ &= \sum_\beta (-1)^\lambda D_{\lambda\beta}^{1*} \hat{d}_\beta^i,\end{aligned}\quad (14)$$

where the subscripts μ and β denote the spherical tensor components in the space- and molecular-fixed frames respectively and $(\epsilon_\lambda)_{-\mu} = \delta_{\lambda,\mu}$. This expansion allows the complete separation of the rotational and electronic parts of the matrix element:

$$\begin{aligned}V_{eg}^{\text{int}} &= -\sqrt{\frac{n\hbar\omega}{2\epsilon_0 V}} \sum_p i^{p+1} (2p+1) j_p(kR/2) \\ &\times \sum_{i\beta F} (-1)^\lambda C_{\lambda 0 \lambda}^{1pF} C_{\beta 0 \beta}^{1pF} \langle \psi_e^{\text{rot}} | D_{\lambda\beta}^{F*} | \psi_g^{\text{rot}} \rangle \\ &\times \langle \psi_e^{\text{el}} | (\hat{\eta}_i)^p \hat{d}_\beta^i | \psi_g^{\text{el}} \rangle.\end{aligned}\quad (15)$$

Here the two rotation matrices, $D_{\lambda\beta}^{1*} D_{00}^{p*}$, have been combined using standard angular momentum theory [5].

B. Explicit form

The appropriate explicit basis states are the hybrid Hund case (c) states [3]

$$\begin{aligned}|a\rangle &\equiv |\gamma j_1 j_2 j \Omega_j J m_j w\rangle \\ &\equiv \sqrt{\frac{2J+1}{4\pi}} D_{m_j \Omega_j}^{J*}(\phi, \theta, 0) |\gamma j_1 j_2 j \Omega_j w\rangle\end{aligned}\quad (16)$$

where L_α , S_α and $\mathbf{j}_\alpha = \mathbf{L}_\alpha + \mathbf{S}_\alpha$ are the orbital, spin and total angular momenta of atom α and $\gamma = \{\gamma_1 \gamma_2\}$ where $\gamma_\alpha = \{\bar{\gamma}_\alpha L_\alpha S_\alpha\}$ with all other necessary atomic quantum numbers specified by $\bar{\gamma}_\alpha$. $\mathbf{j} = \mathbf{j}_1 + \mathbf{j}_2$ is the total electronic angular momentum and $\mathbf{J} = \mathbf{j} + \mathbf{l}$ is the total angular momentum of the atom including rotation \mathbf{l} . The labels m and Ω indicate projections along the space-fixed Oz axis and intermolecular OZ axis respectively, and w represents the gerade ($w = 0$) and ungerade ($w = 1$) symmetry, respectively, of inversion through the center of charge of the molecule.

The evaluation of the dipole operator must be performed in the LS basis under the correct symmetry considerations [4], however the inclusion of $\hat{\eta}_i$ modifies this result. In similar fashion to [3], we use the LS basis of $|\gamma LS \Omega_L \Omega_S w\rangle$, where $\mathbf{L} = \mathbf{L}_1 + \mathbf{L}_2$ and $\mathbf{S} = \mathbf{S}_1 + \mathbf{S}_2$, symmetrized according to

$$\begin{aligned}|\gamma LS \Omega_L \Omega_S w\rangle &= N_{\gamma_1 \gamma_2} [|\gamma_1^A \gamma_2^B LS \Omega_L \Omega_S\rangle_- \\ &+ (-1)^{p_{LS}} |\gamma_2^A \gamma_1^B LS \Omega_L \Omega_S\rangle_-].\end{aligned}\quad (17)$$

Here the A and B indicate the atom to which the orbital configuration γ_i belongs, $N_{\gamma_1 \gamma_2}$ is a normalization factor and $p_{LS} = w_1 + w_2 + L_1 + L_2 - L + S_1 + S_2 - S + N + w$ [6], where w_i refers to the atomic inversion symmetry of γ_i . The subscript ‘-’ indicates that the state has been antisymmetrized with respect to electron permutation:

$$\begin{aligned}|\gamma_1^A \gamma_2^B LS \Omega_L \Omega_S\rangle_- &= \frac{1}{\sqrt{2}} [|\gamma_1^A \gamma_2^B LS \Omega_L \Omega_S; \mathbf{r}_1, \mathbf{r}_2\rangle \\ &- |\gamma_1^A \gamma_2^B LS \Omega_L \Omega_S; \mathbf{r}_2, \mathbf{r}_1\rangle].\end{aligned}\quad (18)$$

When $\Omega_L + \Omega_S = 0$, the states $|\gamma_i^A \gamma_j^B LS \Omega_L \Omega_S\rangle_-$ must also be properly symmetrized with respect to $\hat{\sigma}_v$, the reflection operator of the electronic wave function through a plane containing the intermolecular axis, however this does not affect the action of $(\hat{\eta}_i)^p \hat{d}_\beta^i$ and will be ignored. For the $2s2s$ and $2s2p$ states, the symmetrization reduces to

$$|2s2s\rangle = \frac{1}{2} [1 + (-1)^{w-S}] |(2s)^A (2s)^B 0S0 \Omega_S\rangle_- \quad (19)$$

and

$$\begin{aligned}|2s2p\rangle &= \frac{1}{\sqrt{2}} [(2s)^A (2p)^B 1S \Omega_L \Omega_S\rangle_- \\ &+ (-1)^{1-S+w} |(2p)^A (2s)^B 1S \Omega_L \Omega_S\rangle_-]\end{aligned}\quad (20)$$

Note that the coefficients differ from [4] as we include spin in the symmetrization. From the above, the matrix element of $(\hat{\eta}_i)^p \hat{d}_\beta^i$ in the LS basis is

$$\langle 2s2p | (\hat{\eta}_i)^p \hat{d}_\beta^i | 2s2s \rangle = \frac{d_{\text{at}}}{2\sqrt{2}} [1 + (-1)^{w'+1+S+p}] \delta_{\beta \Omega'_L} \quad (21)$$

where d_{at} is the atomic dipole moment, w' and Ω'_L refer to the excited state and the condition $w - S = \text{even}$ is assumed. The presence of $(-1)^p$ is a direct result of the inclusion of the $(\hat{\eta}_i)^p$ term.

To convert to the original basis (16), the transformation (A.11) of [3] is used. The matrix element of $(\hat{\eta}_i)^p \hat{d}_\beta^i$ in the basis (16) reduces to

$$\begin{aligned}\langle \gamma' j'_1 j'_2 j' \Omega'_j w' | (\hat{\eta}_i)^p \hat{d}_\beta^i | \gamma j_1 j_2 j \Omega_j w \rangle \\ = \frac{1}{2\sqrt{2}} d_{\text{at}} F_{1j\beta\Omega_j}^{j'_1 j'_2 j' \Omega'_j} [1 + (-1)^{w'+1+j+p}]\end{aligned}\quad (22)$$

where

$$\begin{aligned}F_{LS\Omega_L\Omega_S}^{j_1 j_2 j \Omega_j} &= \sqrt{(2S+1)(2L+1)(2j_1+1)(2j_2+1)} \\ &\times C_{m_L m_S m_j}^{LSj} \left\{ \begin{matrix} L_1 & L_2 & L \\ S_1 & S_2 & S \\ j_1 & j_2 & j \end{matrix} \right\},\end{aligned}\quad (23)$$

$\{\dots\}$ is a Wigner 9-j coefficient, and dashed quantities refer to the $2s2p$ state and undashed quantities to the $2s2s$ state.

The matrix element of the rotational part of V_{eg}^{int} is

$$\begin{aligned} & \langle \psi_e^{\text{rot}} | D_{\lambda\beta}^{F*} | \psi_g^{\text{rot}} \rangle \\ &= \iint d\Omega \frac{\sqrt{(2J+1)(2J'+1)}}{4\pi} D_{m'_j\Omega'_j}^{J'} D_{\lambda\beta}^{F*} D_{m_j\Omega_j}^{J*} \end{aligned} \quad (24)$$

Using the properties of the rotation matrices, the integral can be evaluated [5] so that

$$\begin{aligned} & \langle \psi_e^{\text{rot}} | D_{\lambda\beta}^{F*}(\phi, \theta, 0) | \psi_g^{\text{rot}} \rangle \\ &= \sqrt{\frac{2J+1}{2J'+1}} C_{m_j\lambda m'_j}^{JFJ'} C_{\Omega_j\beta\Omega'_j}^{JFJ'}. \end{aligned} \quad (25)$$

The complete matrix element is therefore

$$\begin{aligned} V_{eg}^{\text{int}} &= -\sqrt{\frac{I}{\epsilon_0 c}} \sqrt{\frac{2J+1}{2J'+1}} \sum_p i^{p+1} (2p+1) j_p(kR/2) \\ &\times \sum_{F\beta} (-1)^\lambda C_{\lambda 0 \lambda}^{1pF} C_{\beta 0 \beta}^{1pF} C_{m_j\lambda m'_j}^{JFJ'} C_{\Omega_j\beta\Omega'_j}^{JFJ'} \\ &\times F_{1j\beta\Omega_j}^{j'_1 j'_2 j'_3 \Omega'_j} d_{\text{at}} \frac{1 + (-1)^{w'+1+j+p}}{2} \end{aligned} \quad (26)$$

where I is the laser intensity.

The dipole approximation corresponds to setting $kR = 0$, and therefore, since $j_p(0) = \delta_{p,0}$, to $p = 0$ in equation (26) [7]. The $p = 0$ term of (26) differs from the dipole approximation result by the presence of $j_0(kR/2)$ which varies little over the region of the excited bound levels but does oscillate and decay significantly outside this region. Larger values of p do not contribute strongly in the molecular region due to the small magnitude of $j_p(kR/2)$ for $p \neq 0$ but are significant in the asymptotic region. Lastly, we note that the restriction $\Delta w = \pm 1$ arising from the dipole approximation is broken, as even values of p contribute to couplings to gerade metastable states and odd values of p couple to ungerade metastable states.

III. RESULTS

We first perform the calculations using the same basis states for the σ^- coupling set that are used in [3], i.e. we calculate photoassociation from the gerade metastable $J = 2$ channels to the 0_u^+ , $J = 1$ adiabatic potential that asymptotes to $j = 0$. Unlike the calculations of [3], the asymptotic radiation coupling is zero because the summation over p only contributes for $0 \leq p \leq 4$ and over this finite sum the spherical Bessel functions $j_p(kR) \rightarrow 0$ for $kR \gg p$ and $kR \gg 1$. This means that the dressed state formalism or the R -dependent coupling method need not be employed to solve the equations. However, for consistency between the two calculations, the R -dependent tail-off is introduced exactly as it was used in [3].

The photoassociation profiles represent the spontaneous loss from the excited state and are determined from the loss of unitarity of the S -matrix. The photon

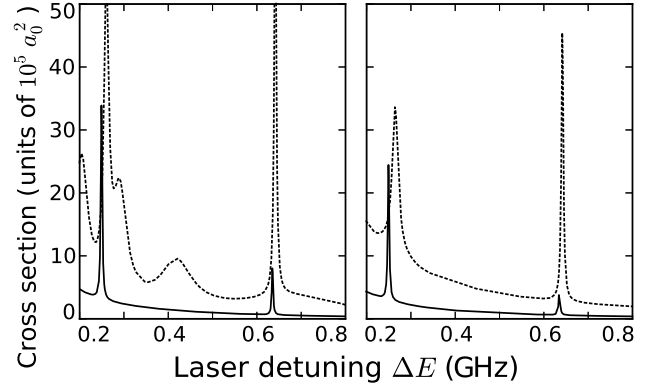


FIG. 1: The photoassociation profiles for intensities of 64 mW/cm^2 (solid line) and 640 mW/cm^2 (dotted line). The left hand plot includes only the $p = 0$ term of the interaction coupling and hence only couplings to gerade metastable states. The right hand plot includes all terms of the p summation and couplings to both gerade and ungerade metastable states.

emission cross section for atoms colliding in the entrance channel $|\alpha\rangle$ is

$$\sigma_\alpha^{\text{photon}} = \frac{\pi}{k_\alpha^2} \left(1 - \sum_{\alpha'} |S_{\alpha'\alpha}|^2 \right) \quad (27)$$

where α and α' enumerate the open channels and k_α is the wavenumber of channel α . The photoassociation profile is then the average

$$\sigma^{\text{photon}} = \frac{1}{n_o} \sum_\alpha \sigma_\alpha^{\text{photon}} \quad (28)$$

where n_o is the number of open channels.

Profiles calculated using only the $p = 0$ contributions are shown in the left hand plot of Fig. 1. The laser interaction term in this case differs from that in the dipole approximation by the presence of $j_0(kR/2)$. From the plot it is evident that, at large laser intensities, there are severe unphysical oscillations in the profiles. Inclusion of all the terms in the p -summation that contribute ($p = 0, 2, 4$) does not noticeably affect the profiles.

To mitigate this problem ungerade $S = 1$ metastable states, normally uncoupled in the dipole approximation, are introduced as open channels. The $p = 1, 3$ terms of the laser coupling contribute to these channels and the total loss profiles for this combination of states are presented in the right hand plot of Fig. 1. These profiles exhibit more expected behavior and possess many similarities to the original PA profiles found using the dipole approximation.

Closer examination however (see Fig. 2) reveals that there is a large difference in behavior between the non-dipole and dipole approximation profiles, especially for high laser intensities. At low intensities the non-dipole profiles show a reduction in the background loss but the resonance peaks have the same shift and width, albeit

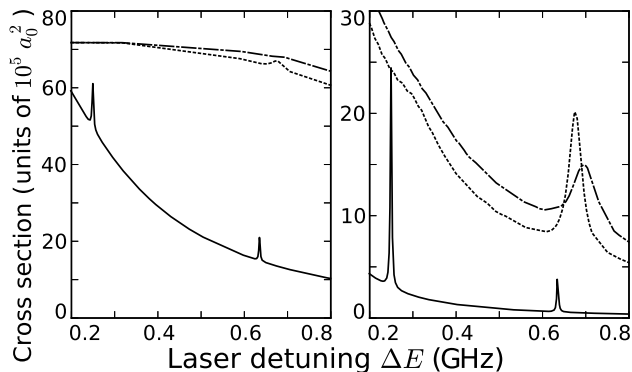


FIG. 2: The photoassociation profiles for intensities of 64 mW/cm² (solid line), 640 mW/cm² (dotted line) and 3.9 W/cm² (dash-dot line). The left hand plot shows profiles that result from the use of the dipole approximation whereas the right hand plot includes the full summation of the non-dipole interaction coupling.

with an increased resonance strength. At higher laser intensities, the resonance parameters still remain identical but the resonances in the non-dipole profiles remain discernable for larger intensities than those in the dipole approximation profiles. In fact, the dipole approximation profiles demonstrate a saturation effect as the background overwhelms the resonance peaks. Instead, in the non-dipole profiles, we observe that the resonance peaks decrease in strength such that the overall loss in the resonance region is smaller at higher intensities. This

suggests possible optical suppression of photoassociative processes at high laser intensities. Why this occurs is unknown, although it is likely due to destructive interference between the ungerade and gerade metastable channels.

The non-dipole coupling also introduces the possibility of more potential photoassociation channels, as the restriction $|J-1| \leq J' \leq |J+1|$ is no longer enforced for summation terms $p \geq 1$. The likelihood that these couplings induce resonances in the excited state potentials is severely suppressed by the spherical Bessel functions as $j_p(kR/2) \ll 1$ for $p \neq 0$ and $kR \ll 1$ (i.e. within the region of bound levels). This prediction was tested by calculating profiles for photoassociation from the $J = 2$ metastable levels to the 0_u^+ , $J = 5$ excited levels and, as expected, no resonances were visible at any laser intensity.

In summary, the PA profiles presented here include all possible coupled metastable levels to the 0_u^+ , $J = 1$ excited state and have been computed without assuming the dipole approximation for the laser coupling. The new calculations using the non-dipole coupling do not modify the resonance parameters that are tabulated in table II of [3] to the accuracy of the calculations. The observed behavior of the background, and the influence of the dipole approximation, are not special to metastable helium but are a result of the weakly bound nature of the excited levels. It would be of much interest if a similar behavior were observed in photoassociation of another atomic species.

[1] H. R. Thorsheim, J. Weiner, and P. S. Julienne, Phys. Rev. Lett. **58**, 2420 (1987)
 [2] J. Weiner, V. S. Bagnato, S. Zilio, and P. S. Julienne, Rev. Mod. Phys. **71**, 1 (1999)
 [3] D. G. Cocks and I. B. Whittingham, Phys Rev. A **80**, 023417 (2009)
 [4] J. Burke, Ph.D. thesis, University of Colorado, 1999.

[5] D. M. Brink and G. R. Satchler, *Angular Momentum*, 2nd ed. (Clarendon Press, Oxford, 1968)
 [6] E. E. Nikitin and S. Ya. Umanskii, *Theory of Slow Atomic Collisions*, 1st ed. (Springer, Berlin, 1984)
 [7] A factor of $-i$ is missing from equation (B16) of [3]